Available online at www.sciencedirect.com
SCIENCE DIRECT®
Physica B 343 (2004) 229–235
PHYSICA B
www.elsevier.com/locate/physb

Critical thicknesses of domain formations in cubic particles and thin films

H. Kronmüller[a,*], D. Goll[a], R. Hertel[b], G. Schütz[a]

[a] Max-Planck-Institut für Metallforschung, Postfach 800665, Heisenbergstrasse 3, Stuttgart D-70569, Germany
[b] Max-Planck-Institut für Mikrostrukturphysik, Weinberg 2, D-06120 Halle, Germany

Abstract

Single-domain, high-remanence particles are the prerequisite for their application in magnetic high-density recording systems. Analytical calculations for the transition between single and multidomain configurations remain unprecise because the calculation of the stray field requires strong simplifications. By means of the three-dimensional finite element method, zero-field magnetization structures of magnetically hard and soft thin film elements and cubic particles have been determined. Numerical results are compared with analytical calculations showing that the latter results depend sensitively on the energy determined for vortex structures.

PACS: 75.75.+a; 75.40.Mg; 75.60.Ch

Keywords: Micromagnetism; Critical thicknesses; Single-domain particles

1. Introduction

The formation of single-domain particles below a critical diameter R of a particle results from a strong decrease of the stray field energy following an R^3-law as compared to an R^2-law due to wall energies of a multidomain state [1–4]. These analytical calculations are usually performed for rotational ellipsoids with axes a and b. By the formation of a two-domain configuration the stray field energy is assumed to be reduced by a factor α, i.e.,

$$\phi_s = \tfrac{1}{2} N_{\|} \mu_0 M_s^2 V \alpha \tag{1}$$

($N_{\|}$: demagnetization factor parallel to the rotational axis b, μ_0: vacuum permeability, M_s: spontaneous magnetization, $V = (4/3)\pi a^2 b$: volume of an ellipsoid with axes a and b). From a comparison of the energies of the single- and the two-domain state, a critical diameter of the rotational ellipsoid is derived as

$$D_{\text{crit}} = \frac{3\gamma}{N_{\|}(1-\alpha)\mu_0 M_s^2}, \tag{2}$$

where γ denotes the wall energy either of Bloch or Néel type. With $\alpha = \frac{1}{2}$, the critical diameter for the Bloch-type wall is given by ($\gamma_B = 4(AK_1)^{0.5}$)

$$D_{\text{crit}}^K = \frac{24\sqrt{AK_1}}{N_{\|}\mu_0 M_s^2} = \frac{12 Q l_K}{N_{\|}}, \tag{3}$$

*Corresponding author. Tel.: +49-711-689-1910; fax: +49-711-689-1912.
E-mail address: kronm@physix.mpi-stuttgart.mpg.de (H. Kronmüller).

0921-4526/$ - see front matter © 2003 Elsevier B.V. All rights reserved.
doi:10.1016/j.physb.2003.08.099

with the quality factor $Q = 2K_1/(\mu_0 M_s^2)$, the exchange constant A and the exchange length $l_K = (A/K_1)^{0.5}$ of the anisotropy constant K_1. In the case of a Néel-type wall in soft magnetic materials with $\gamma_N = 2(2A\mu_0 M_s^2)^{0.5}$ the critical diameter is given by

$$D_{crit}^{s} = \frac{12}{N_{\|}}\sqrt{\frac{2A}{\mu_0 M_s^2}} = \frac{12}{N_{\|}} l_s, \tag{4}$$

with the exchange length, $l_s = (2A/(\mu_0 M_s^2))^{0.5}$, of the stray field. In cases where the transition from a single-domain state to a vortex state takes place, the stray field energy has to be compared with the vortex energy which for a uniaxial material consists of exchange and crystalline energy, given by

$$\phi_v = 2\pi AL \ln(R/l_{s,K}) + \tfrac{1}{2} K_1 \pi R^2 L, \tag{5}$$

where L corresponds to the height of a cylindrical particle of radius R. In the center of the vortex M_s is oriented perpendicular to the plane of the vortex. The extension of this central part is determined by the smallest exchange length, i.e., either l_s or l_K. A similar expression as Eq. (5) has been derived by Hoffmann and Steinbauer [5] using a discrete model. The energy contribution of the central vortex may be omitted if $R \gg l_{s,K}$ holds. The critical diameter of a cylindrical particle then follows from the energy balance between the stray field of the homogeneously magnetized specimen and the vortex state, giving

$$\tfrac{1}{2} N_{\|} \mu_0 M_s^2 R^2 = 2A \ln(R/l_{s,K}) + \tfrac{1}{2} K_1 R^2. \tag{6}$$

2. Size-dependent magnetic configurations

Small particles or thin platelets to be used for magnetic recording systems, e.g., MRAMs, require a more or less homogeneous magnetization configuration. Above some critical size, however, in general a multidomain configuration exists. Analytical calculations of critical thicknesses have been performed by numerous authors [1–7]. In the following, we give a comparison between analytical and numerical results as obtained recently for different particle shapes.

2.1. Cubic particles

Within the framework of the μMAG standard problem No. 3 [8], the critical edge length of a ferromagnetic cube and rectangular platelets has been determined by means of the finite element method [9,10]. In this investigation, it was shown that the quasihomogeneous state at small edge lengths corresponds to a symmetrical flower state. With increasing edge length, a so-called twisted flower state is formed which finally transforms spontaneously into a vortex-type state, initiating the transition to a multidomain state. Fig. 1 shows the dependence of the energy of these three configurations as a function of the edge length of the cube. From this presentation a critical edge length of $D_{crit} = 8.56 l_s$ is derived. These calculations were performed for a quality factor $Q = 2K_1/(\mu_0 M_s^2) = 0.1$. With $\mu_0 M_s = 1$ T and $A = 13$ pJ/m, the material parameters of permalloy, we obtain for the critical thicknesses for Bloch or Néel walls the values $D_{crit}^{K} = 66$ nm and $D_{crit}^{s} = 205$ nm, to be compared with the numerical value of 49 nm. It is obvious from these results that only those based on the Bloch wall-type configurations approach the numerical value.

If we now describe the multidomain configuration by the vortex state we have to solve Eq. (6) with $N_{\|} = \frac{1}{3}$ and $Q = 0.1$, which leads to the

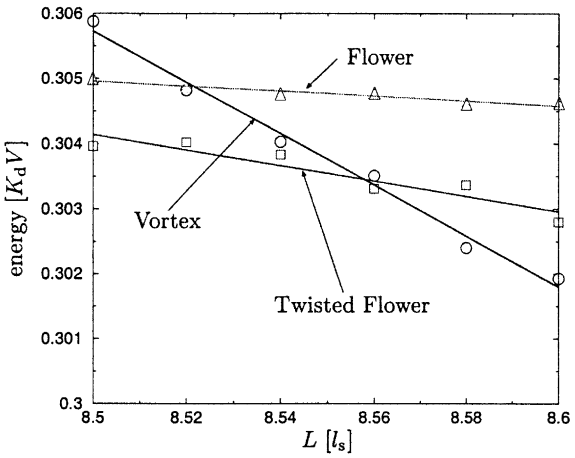

Fig. 1. Size dependence of the total energy of different magnetization states in the ferromagnetic cube in units of $K_d = 0.5\mu_0 M_s^2$ for $Q = 0.1$.

equation

$$0.141 = \ln \varepsilon/\varepsilon^2, \tag{7}$$

where $\varepsilon = R/l_s$. With the solution $\varepsilon = 2.7$ of Eq. (7) and the relation $R = D_{crit}/\sqrt{\pi}$ for the effective radius of a square we obtain $D_{crit} = 4.8 l_s \approx 27.5$ nm to be compared with the numerical result of $D_{crit} = 8.56 l_s$. According to these results, Eq. (3) overestimates D_{crit} and Eq. (6) underestimates D_{crit}. The discrepancy in the case of Eq. (3) is due to an overestimation of the wall energy and in the case of Eq. (6) to the neglect of the stray field energy in the vortex structure which has to be assumed to be fully stray field free. Actually, we deal with a quasivortex which still is charged with a stray field as demonstrated in Fig. 2 where, in particular, the surface charges are shown for different cross-sections. Accordingly, we have to add a stray field energy to the quasivortex structure of Eq. (6) which may be described by a ratio β of the stray field energy of the platelet with respect to that of the homogeneously magnetized cube leading to

$$\tfrac{1}{6}(1-\beta) - 0.025 = \ln \varepsilon/\varepsilon^2. \tag{8}$$

Inserting for ε the numerical result, 4.8, of computational micromagnetism [9], which is compatible with $D_{crit} = \sqrt{\pi} R = 8.56 l_s$, $\beta = 0.44$ is obtained. This result means that the quasivortex still possesses a stray field energy which amounts 44% of the high-remanent state. This result is in fair agreement with the energy contributions obtained by computational micromagnetism [9].

2.2. Square thin platelets

Ferromagnetic nanosquares have been investigated by several authors, mainly with respect to magnetization processes and the switching behavior [11,12]. Critical thicknesses of circular dots were studied by Cowburn [13] and Hoffmann and Steinbauer [5]. The critical thicknesses of rectangular and square platelets in the μm-range have been determined by Hertel [10] and Goll et al. [14]. Fig. 3a–d shows spin configurations of the C- and S-high-remanent states for thicknesses $D = 2$ and 20 nm and an edge length of 1 μm. The reduction of the magnetic inhomogeneity with decreasing

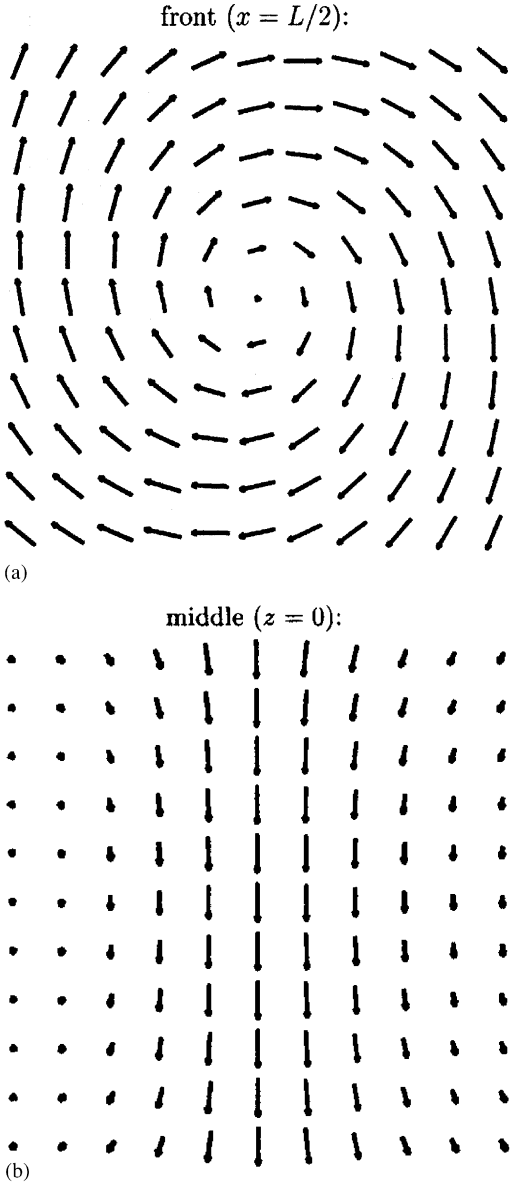

Fig. 2. Vortex state of a cubic particle, projection of the magnetization onto the cross-sections $x = L/2$ and $z = 0$ along the vortex axis.

thickness is quite significant. Fig. 4 shows low-remanent states for permalloy and cobalt for $D = 2$ nm. It is of interest to note that due to the assumed uniaxiality, the vortex-type configuration produces some surface charges on the edges perpendicular to the easy direction even for

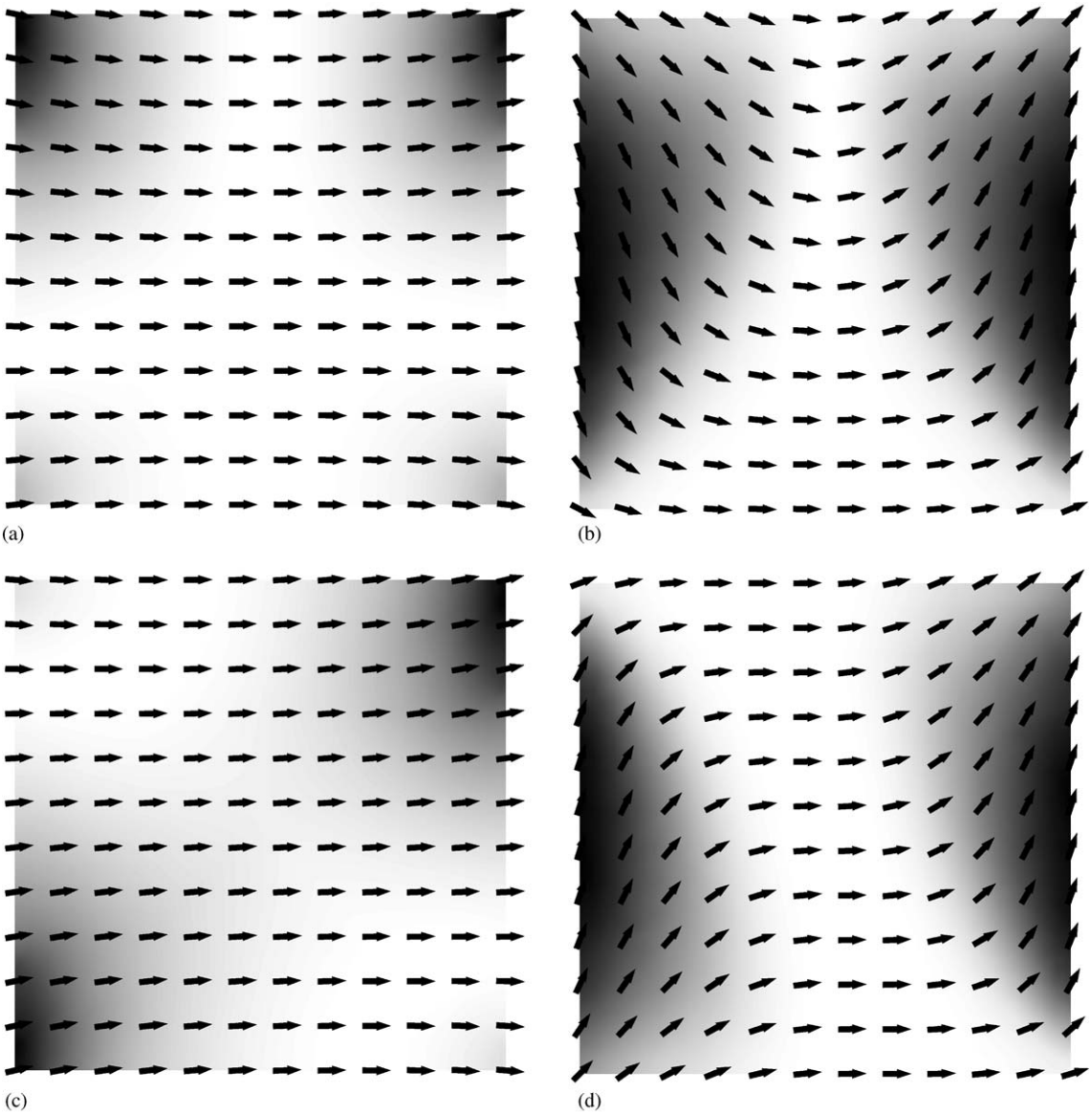

Fig. 3. High-remanent states of C- and S-state configurations obtained by three-dimensional FEM calculations for a square permalloy platelet ($a = 1$ μm): (top left) C-state/2 nm, (top right) C-state/20 nm, (bottom left) S-state/2 nm and (bottom right) S-state/20 nm. Spin configurations are of the platelet's middle-plane deviating only slightly from the surface configurations.

permalloy with its small anisotropy of 5×10^2 J/m^3. In the case of Co with its larger anisotropy constant of $K_1 = 4 \times 10^5$ J/m^3 the vortex-type Landau configuration is replaced by a two-domain laminar domain pattern. Fig. 5 presents for permalloy the total magnetic Gibbs free energies of four different spin configurations—C-state, S-state, flower state and vortex state—as a function of the platelet's thickness and an edge length of $a = 1$ μm. The C-state below 1.8 nm is found to be the energetically most favored configuration. This critical thickness is considerably smaller than l_K or l_s. An analytical calculation of D_{crit} has been performed by

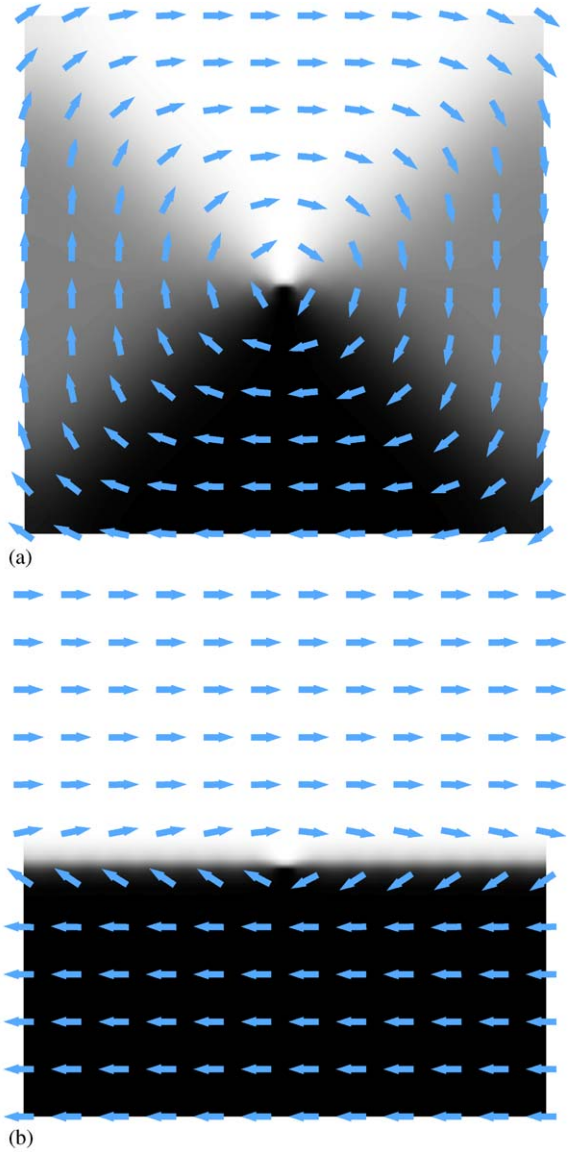

Fig. 4. Low-remanent states of Landau configuration (multi-domain state) achieved by three-dimensional FEM calculations for a square thin platelet ($a = 1$ μm, $D = 2$ nm) of permalloy (left) and cobalt (right). Spin configurations are of the platelet's middle-plane deviating only slightly from the surface configurations.

Goll et al. [14] by comparing the energies of the homogeneously magnetized square with the four domain vortex state. Assuming 90°-Néel walls for the vortex-type state the energy balance may be

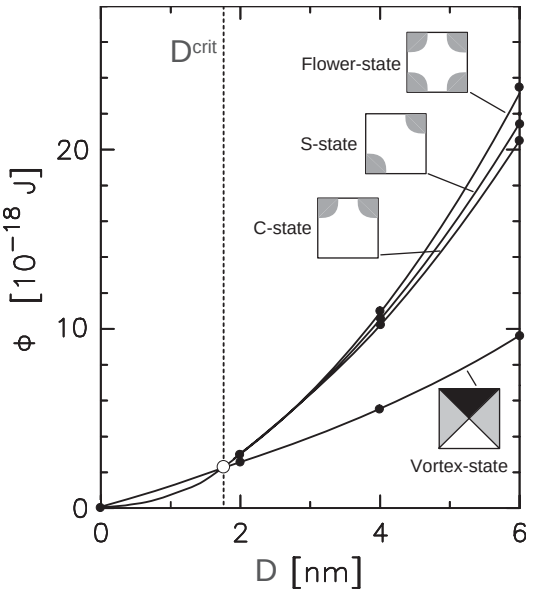

Fig. 5. Total energies Φ obtained by the FEM method for different types of spin configurations in a square permalloy thin platelet of edge length 1 μm as a function of the layer thickness D.

written as [14]

$$\tfrac{1}{2} N_{\parallel} \mu_0 M_s^2 a^2 D = 2\sqrt{2}\gamma_N^{90} a D, \tag{9}$$

$$N_{\parallel} = \frac{1}{2\pi}\left(-\frac{2D}{a}\ln\frac{D}{a} + 1.45\frac{D}{a}\right), \tag{10}$$

$$\gamma^{90} = 0.32\gamma_N^{180}, \tag{11}$$

where γ_N^{180} for thin films is taken from Ref. [4]. $D_{crit} = 0.3$ nm has been obtained, i.e., in drastic difference with the numerical result of 1.8 nm. Using for the vortex-type state the vortex energy of Eq. (5) and taking care of Eq. (10) the energy balance writes

$$\frac{1}{2} N_{\parallel} \mu_0 M_s^2 a^2 D = 2\pi A D \ln\frac{a}{\sqrt{\pi} l_s} + \frac{1}{2} K_1 a^2 D. \tag{12}$$

Rearranging Eq. (12), we finally obtain an implicite equation for D_{crit}

$$-\frac{2D_{crit}}{a}\ln\frac{D_{crit}}{a} + 1.45\frac{D_{crit}}{a} = \frac{4\pi^2 l_s^2}{a^2}\ln\frac{a}{\sqrt{\pi} l_s} + \pi Q. \tag{13}$$

Table 1
Material parameters, hardness Q and exchange lengths l_S and l_K of different magnetic materials

Material	$Ni_{80}Fe_{20}$	Co
J_S (T)	1.0	1.8
K_1 (J/m^3)	5.0×10^2	4.0×10^5
A (pJ/m)	13	13
Q	0.0013	0.310
l_S (nm)	5.7	3.2
l_K (nm)	161.2	5.7

Solving Eq. (13) with the material parameters of permalloy as given in Table 1 gives $D_{crit} = 0.6$ nm. This value is still a factor of 3 smaller than the numerical result and shows clearly that the neglect of the stray field energy in the case of the vortex-type structure leads to a lower bound for the critical thickness. In fact, Fig. 4 clearly shows the existence of surface charges which means that in Eqs. (12) and (13) as for the cube we should add on the right-hand side the contribution of the remaining stray field. Adding a stray field term $\frac{1}{2}N_{\|}\mu_0 M_s^2 a^2 D_{crit}\beta$ the numerical value $D_{crit} = 1.8$ nm is obtained for $\beta = 0.68$. Accordingly, the stray field energy in the case of the vortex-type structure is reduced only by 32% and therefore may not be neglected in agreement with results of the numerical calculations [14]. In soft magnetic materials, the spin structure is predominantly determined by reducing the stray field and in hard magnetic materials mainly the crystal anisotropy is kept small. Therefore, in Co instead of a vortex structure a two-domain structure is formed (Fig. 4b). The balance of energy in this case writes

$$\tfrac{1}{4}N_{\|}\mu_0 M_s^2 a^2 D = \gamma_N^{180} a D, \tag{14}$$

where for thin films according to Goll et al. [14] γ_N^{180} is given by

$$\gamma_N^{180} = 2\pi\sqrt{\sqrt{2}-1}\sqrt{AK_1} + \frac{\pi}{16}\mu_0 M_s^2 D. \tag{15}$$

Inserting Eqs. (15) and (10) for $N_{\|}$ into Eq. (14) leads to the following implicite equation for D_{crit}:

$$-\frac{2D_{crit}}{a}\ln\frac{D_{crit}}{a}\left(\frac{\pi^2}{2} - 1.45\right) = 8\pi^2\sqrt{\sqrt{2}-1}\,Q\frac{l_K}{a}. \tag{16}$$

With the material parameters of Table 1 for Co the solution of Eq. (16) leads for $a = 1$ μm to $D_{crit} = 21$ nm in excellent agreement with the numerical result of Goll et al. [14].

3. Conclusions

The present study of critical thicknesses of cubes and squared platelets has clearly shown that analytical calculations suffer of the difficulty to determine the stray field energy correctly. Therefore, analytical calculations are predominantly suitable to determine upper and lower bounds of critical parameters. Whereas, in the case of the cube the analytical result for D_{crit} using a Bloch-type demagnetized structure leads to suitable results the assumption of a pure vortex-type structure shows larger deviations from the predictions of the numerical calculations. These deviations have to be attributed to the assumption of stray field-free vortex structures. These discrepancies become even more expressed in the case of soft magnetic platelets where the vortex-type structures develop still a considerable stray field energy comparable to the exchange energy. The situation is much better in the case of magnetically hard platelets where a well-defined two-domain pattern leads to values of D_{crit} in agreement with the numerical results.

References

[1] C. Kittel, Rev. Mod. Phys. 21 (1949) 541.
[2] W.F. Brown Jr., J. Appl. Phys. 33 (1962) 3026.
[3] E. Kneller, in: S. Flügge (Ed.), Handbuch der Physik, Vol. XVIII/2, Springer, Berlin, 1966.
[4] A. Aharoni, Introduction to the Theory of Ferromagnetism, Clarendon Press, Oxford, 1996.
[5] H. Hoffmann, F. Steinbauer, J. Appl. Phys. 92 (2002) 5463.

[6] H.F. Schmidts, H. Kronmüller, J. Magn. Magn. Mater. 129 (1994) 361.
[7] W. Rave, K. Fabian, A. Hubert, J. Magn. Magn. Mater. 190 (1998) 332.
[8] R.D. Mc Michael, Standard Problem No. 3, http://www.ctcms.nist.gov/rdm/mumag.html, 1998.
[9] R. Hertel, H. Kronmüller, J. Magn. Magn. Mater. 238 (2002) 185.
[10] R. Hertel, Z. Metallkd. 93 (2002) 10.
[11] L. Torres, L. Lopez-Diaz, E. Martinez, J. Iniguez, Physica B 306 (2001) 112.
[12] J. Fidler, T. Schrefl, W. Scholz, D. Suess, V.D. Tsiantos, Physica B 306 (2001) 112.
[13] R.P. Cowburn, J. Phys. D 33 (2000) R1.
[14] D. Goll, G. Schütz, H. Kronmüller, Phys. Rev. B 67 (2003) 094414-1.